Synthetic Derivatives of (+)- epi -α-Bisabolol Are Formed by Mammalian Cytochromes P450 Expressed in a Yeast Reconstituted Pathway

Arthur Sarrade-Loucheur, Dae-Kyun Ro, Régis Fauré, Magali Remaud-Siméon, Gilles Truan

Research Article

Synthetic Derivatives of (+)-*epi*-α-Bisabolol Are Formed by Mammalian Cytochromes P450 Expressed in a Yeast Reconstituted Pathway

Arthur Sarrade-Loucheur, Dae-Kyun Ro, Régis Fauré, Magali Remaud-Siméon,* and Gilles Truan*

ABSTRACT: Identification of the enzyme(s) involved in complex biosynthetic pathways can be challenging. An alternative approach might be to deliberately diverge from the original natural enzyme source and use promiscuous enzymes from other organisms. In this paper, we have tested the ability of a series of human and animal cytochromes P450 involved in xenobiotic detoxification to generate derivatives of (+)-*epi*-α-bisabolol and attempt to produce the direct precursor of hernandulcin, a sweetener from *Lippia dulcis* for which the last enzymatic steps are unknown. Screening steps were implemented *in vivo* in *S. cerevisiae* optimized for the biosynthesis of oxidized derivatives of (+)-*epi*-α-bisabolol by coexpressing two key enzymes: the (+)-*epi*-α-bisabolol synthase and the NADPH cytochrome P450 reductase. Five out of 25 cytochromes P450 were capable of producing new hydroxylated regioisomers of (+)-*epi*-α-bisabolol. Of the new oxidized bisabolol products, the structure of one compound, 14-hydroxy-(+)-*epi*-α-bisabolol, was fully elucidated by NMR while the probable structure of the second product was determined. In parallel, the production of (+)-*epi*-α-bisabolol derivatives was enhanced through the addition of a supplementary genomic copy of (+)-*epi*-α-bisabolol synthase that augmented the final titer of hydroxylated product to 64 mg/L. We thus demonstrate that promiscuous drug metabolism cytochromes P450 can be used to produce novel compounds from a terpene scaffold.

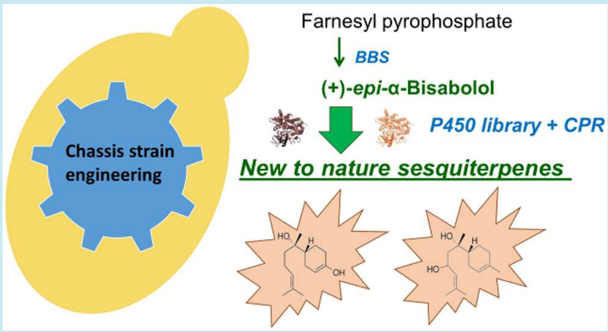

KEYWORDS: *sesquiterpene, Saccharomyces cerevisiae, functional screening, enzyme promiscuity, mixed function oxidases*

Terpenes represent one of the most diverse classes of secondary metabolites comprising more than 50 000 molecules to date.[1] Present in all living kingdoms, their roles range from communication (hormone, abscisic acid), insect attraction, deterrent, and defense molecules in plants to hormones, and signaling compounds in insects,[2,3] and mainly as defense molecules in bacteria and fungi.[4] Terpenes also possess interesting pharmacological activities and are anti-malarial (artemisinin), anticancer (taxol), and anti-inflammatory ((−)-α-bisabolol).[5,6] Many of them also display aromatic properties of major interest for industrial uses (ambroxide, nootkatone, etc.). The vast diversity of terpenes originates from the modularity of their chemical structures. They are synthesized by head to tail condensation of two building blocks composed of five carbons linked to a pyrophosphate group: isopentenyl pyrophosphate (IPP) and dimethylallyl pyrophosphate (DMAPP), leading to geranyl-pyrophosphate (GPP, C_{10}). Condensation of IPP onto GPP leads to farnesyl pyrophosphate (FPP, C_{15}), and further to geranylgeranyl pyrophosphate (GGPP, C_{20}) using another IPP molecule. Terpene synthases can use any of these precursors, by removing the pyrophosphate group while rearranging the carbon backbone and ultimately producing an extremely large diversity of terpene molecules. Most of them can be further functionalized via enzymatic reactions involving oxidative enzymes such as cytochromes P450 (CYP), alcohol dehydrogenases, epoxidases, and other enzyme classes such as glycosyltransferases.[7,8]

Owing to their broad biological and physicochemical properties, terpenes are widely used as commodities despite a low content often found in natural sources. Chemical synthesis of terpenes was thus largely explored but remains challenging due to the presence of chiral centers and/or stereospecific oxidation positions in natural terpenes.[9] To bypass these hurdles, synthetic biologists alternatively implemented metabolic engineering strategies, notably in industrial workhorse microorganisms such as *Saccharomyces cerevisiae* and *Escherichia coli*. Production of terpenes in *S.*

Received: October 1, 2019
Published: January 24, 2020

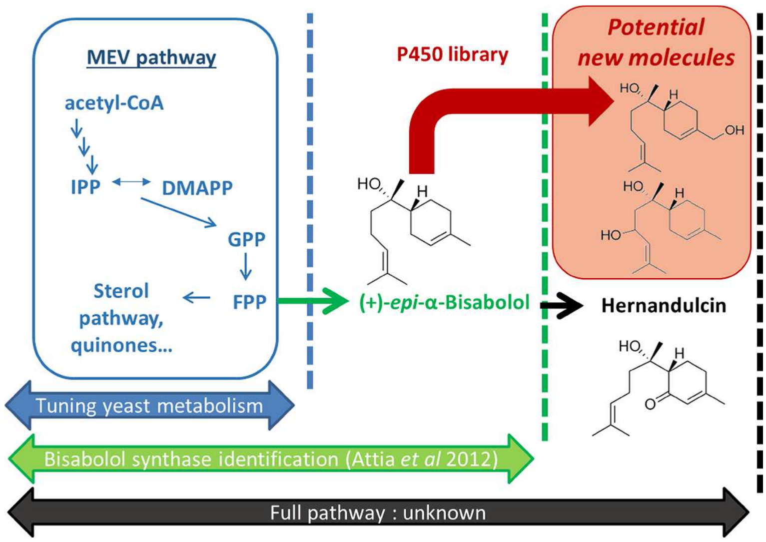

Figure 1. Strategy to produce derivatives of (+)-*epi*-α-bisabolol (including hernandulcin) using the yeast optimized MEV pathway, (+)-*epi*-α-bisabolol synthase, and an *in vivo* screen to unravel oxidative enzymes. IPP, isopentenyl pyrophosphate; DMAPP, dimethylallylpyrophosphate; GPP, geranyl pyrophosphate; FPP, farnesyl pyrophosphate.

cerevisiae and *E. coli* relies on the possibility to branch synthetic terpene pathways onto the MEV or MEP pathways, respectively. In *S. cerevisiae*, optimization of the metabolic flux toward terpene molecules was investigated using the overexpression of a truncated version of the HMG1 gene involved in sterol feedback regulation,[10] overexpression of key enzymes such as ERG20 or downregulation of native competing pathways.[11,12] Building on these strategies, sesquiterpenes including farnesene, nerolidol, and artemisinic acid were produced at the grams per liter scale in both prokaryotes and eukaryotes.[11,13,14]

Identification of natural enzymes of terpene biosynthetic pathways are essentially based on genomics and transcriptomics data mining. As terpene precursors are reasonably well produced in engineered microbial cell factories, the discovery of enzymes involved in the terpene pathway through direct *in vivo* screening has become a viable strategy.[15,16] Furthermore, engineered chassis microorganisms offer the possibility to enlarge the repertoire of natural products by producing new to nature compounds.[17] For example, terpenes absent in their native plant species were obtained from *in vivo* coexpression and/or combination of heterologous enzymes originating from multiple plants[18,19] or obtained via enzyme engineering,[20,21] thus highlighting the potential of these approaches to diversify terpene products.

Hernandulcin is a sesquiterpene derived from (+)-*epi*-α-bisabolol, which was originally isolated from *Lippia dulcis,* a plant from Central America (Figure 1). The pure molecule has attracted interest due to its sweetening properties; 1,000 times sweeter than sucrose. However, its production level *in planta* is rather low[22] and its chemical synthesis involves multiple tedious steps due to the presence of two chiral centers, whereas only one isomer is perceived as sweet.[23] The recent discovery of the (+)-*epi*-α-bisabolol synthase (BBS) converting FPP to (+)-*epi*-α-bisabolol unraveled a critical step in the synthesis of the terpene backbone of hernandulcin, and its activity was validated in *S. cerevisiae*.[24] However, the final oxidation step(s) leading to hernandulcin in *L. dulcis* is (are) still to be discovered although enzymes such as CYPs are considered as serious candidates.

Most plant CYPs involved in secondary metabolism have a rather narrow substrate specificity, rendering the identification of the natural oxidative enzyme(s) from *L. dulcis* highly challenging due to the multiplicity of CYP encoding genes. In contrast, animals possess a limited set of highly promiscuous CYP enzymes responsible for xenobiotic detoxification.[25] Surprisingly, there is no report describing the use of their remarkable oxidative properties to generate natural or new to nature molecules related to the plant secondary metabolism.

Knowing that expression of functional CYPs in engineered yeast is well mastered in our group[26] and that (+)-*epi*-α-bisabolol can be directly produced by *S. cerevisiae*, we assessed the ability of animal CYPs to convert (+)-*epi*-α-bisabolol into hernandulcin or related molecules (Figure 1). Furthermore, as α-bisabolol has anti-inflammatory properties and can potentiate some antibiotic effects, we hypothesized that (+)-*epi*-α-bisabolol oxidation by various drug metabolism CYPs could generate other derivatives of interest, not only regarding their sweetness potency as sole biological feature but also for potential pharmaceutical properties.[5,27] Indeed, some human CYPs are competitively inhibited by α-bisabolol suggesting that the latter can enter the active site and potentially act as an undescribed substrate,[28] and we hypothesized the same behavior for (+)-*epi*-α-bisabolol. Our in house-generated library of CYPs was thus used together with a suitable cytochrome P450 reductase (CPR) in the genome of *S. cerevisiae* to assess their ability to produce new derivatives. In parallel we pointed out an imbalance in the designed pathway and improved the production of the desired molecules by adding an extra copy of BBS.

■ MATERIALS AND METHODS

Materials. Diclofenac, (−)-α-bisabolol, *trans,trans*-farnesol, *trans*-nerolidol, and nootkatone were purchased from Sigma-Aldrich (Munich, Germany), and 4-hydroxy-diclofenac was obtained from Bertin Bioreagent (Montigny le Bretonneux, France). The racemic (±)-hernandulcin chemical standard (*R*/

Table 1. Plasmids Used in This Study

plasmid name	cloned enzymes	origin of replication	promoter	terminator	yeast marker	source
pESC-Leu2d + CPR + BBS	BBS + Aa CPR	2μ	GAL1/GAL10	CYC1	Leu2	described in ref 24
pMRI31		integrative in HO locus	GAL1/GAL10	CYC1/ADH1	KanMX	described in ref 33
pMRI32		integrative in Ty4 locus	GAL1/GAL10	CYC1/ADH1	KanMX	described in ref 33
pMRI34		integrative in DPP1 locus	GAL1/GAL10	CYC1/ADH1	KanMX	described in ref 34
pMRI31H + BBS	BBS + Hs CPR	integrative in HO locus	GAL1/GAL10	CYC1/ADH1	KanMX	this study
pMRI31S + BBS	BBS + Sc CPR	integrative in HO locus	GAL1/GAL10	CYC1/ADH1	KanMX	this study
pMRI32H + BBS	BBS + Hs CPR	integrative in Ty4 locus	GAL1/GAL10	CYC1/ADH1	KanMX	this study
pMRI32S + BBS	BBS + Sc CPR	integrative in Ty4 locus	GAL1/GAL10	CYC1/ADH1	KanMX	this study
pMRI34S − BBS	BBS + Sc CPR	integrative in DPP1 locus	GAL1/GAL10	CYC1/ADH1	KanMX	this study
pMRI34S + BBS	BBS + Sc CPR	integrative in DPP1 locus	GAL1/GAL10	CYC1/ADH1	KanMX	this study
pSH47	Cre	ARSH4−CEN6	GAL1	CYC1	Ura3	Euroscarf (Scientific Research and Development GmbH, Oberursel, Germany)
pYEDP60		2μ	GAL10-CYC1 hybrid promoter	PGK	Ura3	described in ref 35
pYEDP60 + CYP	CYP library (Table S1)	2μ	GAL10-CYC1 hybrid promoter	PGK	Ura3	in house

Table 2. Strains Used in This Study

strain name	genotype	origin
Top10	F- mcrA Δ(mrr-hsdRMS-mcrBC) Φ80lacZΔM15 Δ*l*acX74 recA1 araD139 Δ(ara-leu)7697 galU galK rpsL (StrR) endA1 nupG	Thermo Fischer Scientific (Waltham, MA, US)
BY4741	MATa his3Δ1 leu2Δ0 met15Δ0 ura3Δ0	Euroscarf
EPY300	MATα his3Δ1 leu2Δ0 lys2Δ0 ura3Δ0 PGAL1−tHMG1: :δ1 PGAL1−upc2−1: :δ2 erg9: :PMET3−ERG9: :HIS3 PGAL1−ERG20: :δ3 PGAL1−tHMG1: :δ4	described in ref 31
YBIS_01	EPY300, Δho::TADH1-BBS-PGAL10-PGAL1-ScCPR-TCYC1	this study
YBIS_02	EPY300, Δho::TADH1-BBS-PGAL10-PGAL1-HsCPR-TCYC1	this study
YBIS_03	EPY300, Δ*Ty4*::TADH1-BBS-PGAL10-PGAL1-ScCPR-TCYC1	this study
YBIS_04	EPY300, Δ*Ty4*::TADH1-BBS-PGAL10-PGAL1-HsCPR-TCYC1	this study
YBIS_05	EPY300, Δho::TADH1-BBS-PGAL10-PGAL1-ScCPR-TCYC1, ΔDPP1:: TADH1- -PGAL10-PGAL1-ScCPR-TCYC1	this study
YBIS_06	EPY300, Δho::TADH1-BBS-PGAL10-PGAL1-ScCPR-TCYC1, ΔDPP1:: TADH1-BBS-PGAL10-PGAL1-ScCPR-TCYC1	this study

R, *S*/*S*) was purchased from Synphabase (Pratteln, Switzerland). DNA polymerases and restriction enzymes were supplied from New England Biolabs (Ipswich, MA, US) and Thermo Fischer Scientific (Waltham, MA, US). Primers were ordered at IDT (Coralville, IA, US), and sequencing was performed using Eurofins (Luxembourg, Luxembourg). For microbial cultures, peptone was from MP Biomedicals (Santa Ana, CA, US), tryptone, yeast extract, yeast nitrogen base, and amino acid mixtures were from Formedium (Hunstanton, UK). Yeast microsomal fractions coexpressing CPR and the human CYPs in yeast were supplied by Bertin Pharma (Montigny le Bretonneux, France), while CYP2B11 microsomal fractions were prepared as previously described.[29]

Microbial Strains. The yeast strains used in this study are based on the S288C genetic background[30] and EPY300 is a chassis strain of *S. cerevisiae* engineered to trigger FPP accumulation and optimize the mevalonate pathway flux.[31,32] Additional genomic integrations were performed using the pMRI31-32-34 vectors listed in Table 1 to generate the strains listed in Table 2.

CYP Library. The CYPs encoding genes were inserted in the multicloning site of pYEDP60 under the control of the GAL10-CYC1 hybrid promoter.[35] The list of the cloned CYPs is described in Table S1.

Plasmid Construction. All cloning and plasmid amplification steps were performed in TOP10 *E. coli* cells. The coding sequence of BBS was amplified using primer 1 and 2 with Phusion polymerase and pESC-Leu2d + CPR + BBS as template for 30 cycles (primers in Table S2). The resulting PCR product was digested by EcoRI/BglII and inserted in the GAL10 promoter of pMRI31 and pMRI32. Then *S. cerevisiae* or *H. sapiens* CPR (UniprotKB numbers P16603 and P16435, respectively) coding sequences were amplified by PCR using primers 3−4 and 5−6 and inserted in the GAL1 promoter of pMRI31 + BBS or pMRI32 + BBS using BamHI /SalI restriction sites, leading to the plasmids pMRI31H + BBS, pMRI31S + BBS, pMRI32H + BBS, pMRI32S+BBS (Table 1). For pMRI34S + BBS, the cassette comprising BBS and CPR coding genes was digested from pMRI31S + BBS using PacI and SalI restriction enzymes and cloned in the pMRI34 backbone. The plasmid pMRI34S − BBS was constructed from the plasmid pMRI34S + BBS by PCR amplification and using primers 7 and 8, which allowed the removal of the BBS coding sequence.

Plasmid Transformation and Integration of DNA Cassettes in Yeast. The lithium acetate method was applied for yeast transformation with replicative plasmids.[36] When genomic integrations were carried out, the integrative vectors were linearized and transformed.[37] After obtaining clones resistant to geniticin (400 μg/mL), integration at the desired locus was checked by colony PCR. After transformation or integration, the respiration ability of each yeast strain was checked by streaking the strain on a non-fermentable growth media N3 (2% peptone (w/v), 1% yeast extract (w/v), and 3% glycerol (w/v)).

When successive rounds of integrations were needed, recycling of the KanMX cassette was performed by transforming the pSH47 plasmid expressing Cre recombinase.[38] The Cre recombination event was selected by screening geniticin sensible clones, and the curation of pSH47 plasmid was selected by the recovery of Ura^- clones. Before the second integration of the pMRI34 plasmids, the (+)-*epi*-α-bisabolol productivity was verified to ensure that potential deleterious genetic events did not occur during marker excision.

Strain Culture Conditions and Sampling. For production of (+)-*epi*-α-bisabolol with the different strains, precultures were inoculated in SD medium (synthetic complete drop-out medium with 2% glucose (w/v), yeast nitrogen base + ammonium sulfate 6.9 g/L) and a mixture of all amino acids except those used for plasmid selection. In addition, EPY300 and derivative strains were grown without histidine to ensure genetic stability and without methionine to avoid repression of ERG9 by MET3 promoter. Precultures were grown overnight at 30 °C under 200 rpm stirring. Using these seed precultures, cultures were then inoculated at 0.1 $OD_{600\ nm}$ either in SD medium or in YPA medium containing 20 g/L peptone, 10 g/L yeast extract, and 80 mg/L adenine). Both media were supplemented with 0.4% glucose (w/v) and 1.6% galactose (w/v) for induction, and 2 mM methionine (ERG9 repression). A dodecane overlay representing 10% (v/v) of the culture was used to enhance (+)-*epi*-α-bisabolol secretion when mentioned.

To produce hydroxylated (+)-*epi*-α-bisabolol metabolites, a preculture was grown overnight in SD medium -His-Met-Ura at 200 rpm and 30 °C, and used to inoculate 0.1 $OD_{600\ nm}$ YPA medium supplemented with 0.4% glucose (w/v), 1.6% galactose (w/v), and 2 mM methionine. The cultures were grown at 160 rpm and 30 °C. Samples of 5 mL of culture broth and cells were taken after 120 h of incubation and kept at −20 °C until extraction.

To check that chassis strains are suitable for CYPs screening, a diclofenac bioconversion experiment was conducted using 1 mM diclofenac. Diclofenac was added at the beginning of the culture done in the same conditions as those used for hydroxylated (+)-*epi*-α-bisabolol products.

Cell dry weights were determined from 5 mL of culture broth samples that were filtered, washed with 0.1 N HCl under a vacuum pump, and dried in a desiccator chamber (at 60 °C under vacuum) before weighing.

Metabolite Extraction and Analytical Detection of the Sesquiterpenes. When a dodecane overlay was used during cultivation, cultures were centrifuged at 8 000*g* for 10 min at ambient temperature to separate dodecane from culture broth. The absence of any effect upon the addition of the internal standard addition to the dodecane overlay while inducing the culture was verified (data not shown). The dodecane fraction was directly injected in GC equipped with FID and MS detection after dilution when required. GC-FID−MS module Trace1310 and ISQ LT (Thermo Scientific) were used to quantify (+)-*epi*-α-bisabolol, farnesol, and nerolidol, and nootkatone as internal standard using N_2 as carrier gas. The inlet was fixed at 200 °C and samples were injected on TG-5MS column (Thermo Scientific) and then eluted using a linear gradient starting at 40 °C and ramping up to 250 °C in 21 min with a final step at 250 °C held for 9 min.

In the absence of dodecane overlay, 5 mL samples of culture broth were taken and mixed with 1 g of glass beads (θ = 0.4 μm−0.6 μm, acid washed beads, Sigma-Aldrich) and 2.5 mL of hexane. This mix was vortexed 1 min in order to disrupt yeast cell wall and membrane and ensure the transfer of the hydrophobic molecules to the solvent phase. Then, the mixture was centrifuged at 10 000*g* for 10 min at ambient temperature. The solvent fraction was collected, and the extraction was repeated a second time. After solvent evaporation under airflow, the samples were suspended in 0.5 mL of pure ethanol and injected in a HPLC−UV−MS or in GC-FID−MS. HPLC was performed using a Waters HPLC 2790 separation module equipped with a C_{18} precolumn and a Prontosil 120-5-C18-SH 5.0 μm 250 mm × 4.0 mm column (Bischoff chromatography). An elution gradient was applied at a constant flow rate of 0.75 mL/min using solvent A (water + 0.03% formic acid (v/v)) and B (acetonitrile + 0.03% formic acid (v/v)). Gradient started at 85% A (v/v) and 15% B (v/v) for 3 min, ramping up to 100% B over 24 min then held for 5.5 min at 100% B. (+)-*epi*-α-Bisabolol and (+)-*epi*-α-bisabolol derivatives were detected at 205 nm, using a Waters 996 photodiode array detector (Waters). For mass spectrometry detection, a Micromass ZQ module (Waters) was used using ESI^+ ionization and a capillary voltage of 3.5 kV and a cone set at 30 V, masses were scanned in a range spanning 150 to 350 Da.

For the diclofenac bioconversion experiment, 0.5 mL of the culture medium were acidified with 5 μL of 1 M HCl, and then mixed with 0.5 mL of acetonitrile and glass beads. The mix was vortexed 1 min, centrifuged at 16 000*g* for 5 min and directly injected in HPLC. The gradient started at 85% A (v/v) and 15% B (v/v) for 3 min, ramping up to 100% B over 24 min, and then was held for 5.5 min at 100% B. Diclofenac was quantified at 276 nm and 4-hydroxy-diclofenac at 267 nm.

Enzymatic Assays with CYP Microsomal Fractions. Reactions were set up with microsomal fractions in a 50 μL volume containing 1.2 mM NADPH, 400 μM (−)-α-bisabolol or farnesol or nerolidol (10 mM solubilized in DMSO), 50 nM CYP microsomal fractions in 50 mM Tris-HCl pH 7.5, and 1 mM EDTA. The reactions were stopped after 5 min or one hour incubation at 30 °C by adding one volume of acetonitrile and vortexing. Finally, the assay was centrifuged at 16 000*g* for 5 min at ambient temperature before HPLC−UV−MS analysis. The HPLC method was optimized for the analysis of the (−)-α-bisabolol oxidized products in order to improve their separation even if the products still were not completely separated using this gradient. Gradient started at 85% A (v/v) and 15% B (v/v) for 3 min, ramped up to 65% B in 4 min, reached 90% B over a 20 min gradient, and then was held for 5.5 min at 100% B.

Isolation and Characterization of the Bisabolol Oxidation Products. The strains YBIS_06 + CYP2B6 or

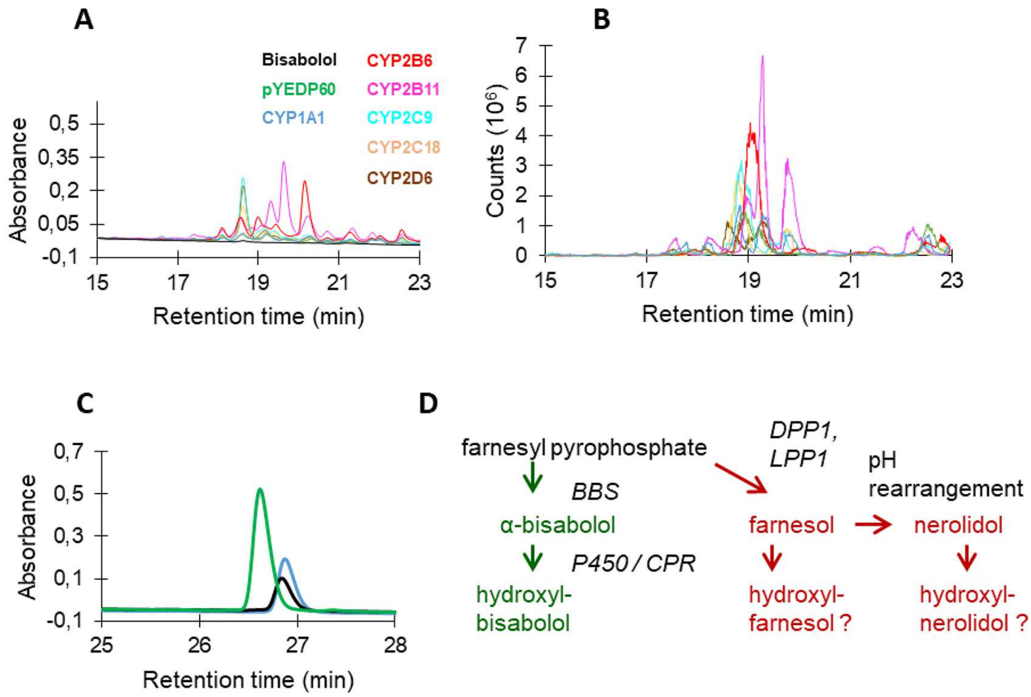

Figure 2. Detection of new molecules generated in the YBIS_01 strain transformed by the empty plasmid pYEDP60, or by some CYPs. (A) UV chromatogram (205 nm). (B) Mass spectrometry signal showing signal at m/z = 203.3 corresponding to hydroxylated (+)-*epi*-α-bisabolol molecules in accordance with Figure 2A chromatograms. (C) HPLC-UV chromatograms of (−)-α-bisabolol blue trace, farnesol green trace, and nerolidol black trace. (D) Potential off target oxidation routes derived from (+)-*epi*-α-bisabolol isomers that may exist *in vivo* in the chassis strain.

CYP2B11, CYP2C9, CYP2D6 showing accumulation of (+)-*epi*-α-bisabolol oxidation products were grown in 5 L Erlenmeyer flask using 1 to 2 L culture volumes. First, a seed culture of 5 mL in SD-His-Met-Ura was inoculated at 30 °C, 200 rpm overnight, and served to start a second preculture of 50 mL in the same conditions. Then a culture of 1 to 2 L was inoculated at 0.1 $OD_{600\ nm}$ YPA medium supplemented with 0.2% glucose (w/v), 1.8% galactose (w/v), and 2 mM methionine. The culture was harvested after 5 days, centrifuged at 6 000*g* for 25 min at ambient temperature. The whole supernatant was then applied on a preparative column filled with 20 g of octadecyl-functionalized silica gel (Sigma-Aldrich). The column was washed with 400 mL of water containing 10% ethanol (v/v). (+)-*epi*-α-Bisabolol oxidized derivatives were then eluted with 100 mL of pure ethanol, filtered on a Buchner funnel and concentrated under vacuum. The oily fraction was purified on a silica cartridge (HP silica 20 μm) using an automated Reveleris flash chromatography system (Grace) with a gradient of ethyl acetate in hexane. The recovered fractions were injected on HPLC−UV−MS and analyzed in the same conditions as those described above to verify the purity of each compound.

The hydroxylated metabolites of (+)-*epi*-α-bisabolol were then characterized by NMR. NMR spectra were recorded at 298 K on a Bruker Avance II spectrometer at 500 and 125 MHz for ^{1}H and ^{13}C respectively. Coupling constants (J) are reported in Hz, and chemical shifts (δ) are given in ppm with the residual solvents signal as internal reference. Multiplicities are reported as follows: s = singlet, d = doublet, t = triplet, m = multiplet, and br = broad. Analysis and assignments were performed using 1D (^{1}H, ^{13}C, Jmod, and selective TOCSY) and 2D (COSY, TOCSY, HSQC, and HMBC) experiments.

Trimethylsilylation of the (+)-*epi*-α-bisabolol hydroxylated products was carried out using bis(trimethylsilyl)-acetamide/trimethylchlorosilane (5/1, v/v) (Sigma-Aldrich) by adding one volume of the products extracted from the culture broth in hexane to one volume of silylation agent. The reaction was incubated 30 min at 50 °C and analyzed by GC−MS as described above.

■ RESULTS

Building an Efficient Chassis Strain for Screening (+)-*epi*-α-Bisabolol Hydroxylation by CYPs. *In vivo* screening of CYPs capable of (+)-*epi*-α-bisabolol oxidation in yeast requires a convenient strain. Hence, we compared the wild-type strain BY4741 to EPY300,[32] a previously optimized strain for terpene production relying on the same S288C genetic background. BBS was expressed from the high copy number plasmid pESC leu2D BBS + CPR. After growth in a biphasic culture with a dodecane overlay, (+)-*epi*-α-bisabolol was only detected in the engineered EPY300 strain, indicating that a strain optimized for sesquiterpene production is indeed a prerequisite for *in vivo* screening purposes (Figure S1). To select animal CYPs enzymes active on (+)-*epi*-α-bisabolol, further modifications of the engineered strain EPY300 were required, notably the overexpression of yeast or human CPR, as previously described.[26] To ease subsequent screening of the plasmid expressing the CYP, the two CPR genes were separately integrated, under the control of a strong, inducible promoter (GAL1, in the genome of *S. cerevisiae*.

The genome integration of BBS and CPR genes under the control of GAL10 and GAL1 was performed in EPY300, at locus HO (strains YBIS_01 (yCPR)/YBIS_02 (hCPR)) or Ty4 (YBIS_03 (yCPR)/YBIS_04 (hCPR)) (Table 2). In

Table 3. *In Vitro* Activities of the CYPs toward (−)-*α*-Bisabolol, Farnesol, and Nerolidol[a]

	CYP1A1		CYP2B6		CYP2B11		CYP2C9		CYP2C18		CYP2D6	
	P	*C*	*P*	*C*	*P*	*C*	*P*	*C*	*P*	*C*	*P*	*C*
bisabolol	±[b]	0	2	0.64	+++[c]	0.72	3	0.65	2	0.24	±[b]	0
farnesol	1	0.05	2	0.15	+++[c]	0.57	1	0.01	1	0.05	±[b]	0
nerolidol					1	0.55	2	0.10	1	0.10	±[b]	0

[a]Notation: *P*, number of detected products; *C*, conversion after 1 h of reaction. Conversion was calculated as the ratio between the area of product(s) and the sum of the areas of substrate and product(s) according to UV quantitation. [b]Trace activities corresponding to a product formation only detectable in MS (see Figures S5−S7). [c]Multiple products are evidenced by HPLC but counting single products is not feasible (see Figures S5−S7). In the absence of available standards, we assumed that substrates and products have a similar molar extinction coefficient at 205 nm.

YBIS_01, the (+)-*epi*-*α*-bisabolol production reached 0.176 mM in the dodecane layer and a similar production level was obtained in YBIS_03 (data not shown). Hence, only the YBIS_01 and YBIS_02 strains (integration at HO) were further used as chassis strains. Additionally, the overexpression of both CPR genes did not cause any measurable toxicity as the growth of both strains was equivalent to that of EPY300.

Overexpression of both CPR was evidenced using the bioconversion of diclofenac to 4-hydroxy-diclofenac by CYP2C9.[39] The basal level of expression of the endogenous yeast CPR of the EPY300 strain sustained a very low activity of CYP2C9, which converted 0.33% of the substrate in 120 h. On the contrary, strains YBIS_01 (yCPR) and YBIS_02 (hCPR), efficiently transformed diclofenac with conversion rates of 98% and 44%, respectively (Figure S2). As already reported with human CYPs the overexpression of *S. cerevisiae* CPR resulted in a higher specific activity of CYP2C9 compared than that obtained using the *H. sapiens* enzyme.[26]

Thus, strain YBIS_01, producing significant amounts of (+)-*epi*-*α*-bisabolol while harboring an optimized redox environment compatible with millimolar conversion of human CYP substrate, was retained as a competent chassis strain for the *in vivo* screening of (+)-*epi*-*α*-bisabolol oxidation activities by drug metabolism CYPs.

***In Vivo* Screening of the CYP Library in the Engineered Strain.** We then implemented the screening of our CYP library, which contains 25 different CYPs, 13 from *H. sapiens*, 8 from other animals, and 4 additional mutants generated from human CYPs (Table S1). After individual transformation of the YBIS_01 strain, each strain was analyzed for the potential production of hydroxylated forms of (+)-*epi*-*α*-bisabolol. Detection of hernandulcin using GC remains tedious due to its thermal lability.[22,40] As hydroxylated products of (+)-*epi*-*α*-bisabolol may also be prone to instability during GC analysis, we relied on a HPLC−UV−MS protocol for screening the CYPs library.

As there is no commercially available (+)-*epi*-*α*-bisabolol standard, (−)-*α*-bisabolol (molecular weight: 222.3 g/mol) was used as the standard for quantitation, assuming that both isomers possess a similar molar extinction coefficient at 205 nm. (−)-*α*-Bisabolol gave a strong MS signal at m/z = 205.3 corresponding to a dehydrated rearrangement ($M + H^+ - H_2O$ = 205.3), which is often observed with hydroxylated products.[41]

HPLC−UV−MS analysis of the culture supernatant from individual clones of our library was then undertaken. We assumed that monohydroxylated or epoxy compounds generated from (+)-*epi*-*α*-bisabolol (molecular weight of 238.3 g/mol) should produce ions at m/z equivalent to $M + H^+ - H_2O$ = 221.3 or $M + H^+ - 2H_2O$ = 203.3. Indeed, we identified such ions for the strains expressing human CYP1A1, CYP2B6, CYP2B11, CYP2C9, CYP2C18, or CYP2D6 albeit with low levels for the latter. Conversely, these two ions were never detected in the strain transformed by the void vector pointing that such metabolites are produced by CYP activities and therefore their molecular weight corresponds to the mass of (+)-*epi*-*α*-bisabolol plus one oxygen atom. Overall, the generated molecules showed UV spectral properties similar to the (+)-*epi*-*α*-bisabolol precursor with an absorbance maximum at 205 nm. The chromatograms of the various strains are shown in Figure 2A for UV and in Figure 2B for m/z ($M + H^+ - 2H_2O$) = 203.3. This ion was the dominantly detected one for the new metabolites using our MS settings while the signal at m/z ($M + H^+ - H_2O$ = 221.3) was weaker. Regarding the low production of new metabolites with CYP2D6, we attempted to improve the production level of oxidized (+)-*epi*-*α*-bisabolol product by placing the open reading frame of the CYP2D6 gene in different codon initiation environments. The best level of oxidized compounds was obtained using an optimized Kozak environment (CYP2D6 H1, Table S1 and Figure S3), which was then systematically used throughout the study. In addition to monohydroxylated products, we also searched for the potential formation of a keto group ($MW_{bisabolol}$ + 14) as occurring in hernandulcin. The racemic form of (±)-hernandulcin (*R*/*R*, *S*/*S*) yielded a peak at m/z = 219.3 corresponding to a dehydrated rearrangement. A thorough analysis of the extracts of the various strains did not show any peak with such a m/z value, indicating that neither hernandulcin nor any keto derivatives of (+)-*epi*-*α*-bisabolol were produced or stable enough to be detected. We also did not detect either any dihydroxylated products with m/z = 254.3 ($MW_{bisabolol}$ + 32) or giving potential rearrangement products ($M + H^+ - H_2O$ = 237.3 or $M + H^+ - 2H_2O$ = 219.3 or $M + H^+ - 3H_2O$ = 201.3).

In the different strains, (+)-*epi*-*α*-bisabolol was detected within a region containing several not well resolved peaks. It is therefore possible that endogenous molecules of close retention times to that of (+)-*epi*-*α*-bisabolol are present in the cell extracts. If such molecules possess the same MW and are hydroxylated by our CYP library, they would be counted as false positive hits and would probably elute in the same region as (+)-*epi*-*α*-bisabolol products. Indeed, in cases where sesquiterpene synthases could not totally convert FPP into sesquiterpenes, dephosphorylation of FPP led to farnesol, a (+)-*epi*-*α*-bisabolol isomer.[42] In our conditions, the resolution of our HPLC−UV−MS method was not sufficient to allow a separation between (−)-*α*-bisabolol chemical standard, farnesol, and nerolidol, thus leading to a probable coelution of their hydroxylated products if they would be produced in our strains (Figure 2C). A further analysis of the sesquiterpenes from YBIS_01 by GC−MS indeed revealed the presence of farnesol and nerolidol (Figure S4).

In the absence of chemical standards for either hydroxylated (+)-*epi*-α-bisabolol, farnesol, or nerolidol derivatives, solid conclusions on the specificity of the tested CYP toward the sesquiterpenes solely based on our primary *in vivo* screening experiments could not be drawn (Figure 2D). This prompted us to verify that the identified CYP enzymes are consistently active with α-bisabolol, farnesol, and nerolidol as substrates via an enzymatic *in vitro* reaction.

***In Vitro* Activities of the Human CYPs with (+)-*epi*-α-Bisabolol, Farnesol, and Nerolidol.** To verify whether the selected CYPs had genuine activities on (+)-*epi*-α-bisabolol rather than farnesol or nerolidol, *in vitro* enzyme assays were conducted. Because of the absence of a commercial source of (+)-*epi*-α-bisabolol, the diastereoisomer (−)-α-bisabolol was used as a surrogate substrate, assuming that both molecules would have comparable binding properties. Enzymatic tests were performed at the same concentration of substrate (0.4 mM). Enzymatic assays of the identified CYPs confirmed that all selected enzymes were active with either some or all sesquiterpenes (Table 3). For each of the tested molecules, the number of detected products and the corresponding conversion yields are listed in Table 3, while the original chromatograms of the enzymatic assays are presented in Figures S5−S8.

CYP1A1 converts farnesol more efficiently than (−)-α-bisabolol as evidenced by the very low levels of hydroxylated compounds with (−)-α-bisabolol, indicating that *in vivo*, farnesol is preferentially oxidized. CYP2D6 shows only weak activities toward the three substrates in the tested conditions even if the *in vivo* accumulation sesquiterpene oxidized products was clearly shown in our chassis strain. CYP2B6, CYP2C9, and CYP2C18 oxidized (−)-α-bisabolol 2.4 to 6-fold more efficiently than farnesol or nerolidol. Therefore, one can expect that, in the chassis strain, the formation of (+)-*epi*-α-bisabolol oxidized products is favored. With CYP2B11, conversion of the three sesquiterpenes is in the same range, and thus, *in vivo*, oxidized derivatives may originate from (+)-*epi*-α-bisabolol, farnesol, and nerolidol. Interestingly, the different CYPs exhibited distinctive patterns of oxidized products from (−)-α-bisabolol; CYP2C18 and CYP2B6 led to two compounds while CYP2B11 and CYP2C9 catalyze the formation of a more diverse range of products.

Structural Characterization of Some (+)-*epi*-α-Bisabolol Derivatives. *Improving (+)-epi-α-Bisabolol Production in Chassis Strain.* Sesquiterpene production can be modulated by several factors, including biphasic culture with dodecane,[31] pH of the medium,[43] the presence of endogenous phosphatases,[42,44] and finally the copy number of the sesquiterpene synthase encoding genes. We thus assessed potential improvements of the (+)-*epi*-α-bisabolol production by modifying the balance of the FPP flux toward (+)-*epi*-α-bisabolol, farnesol, and nerolidol.

(+)-*epi*-α-bisabolol, farnesol, and nerolidol were quantified by GC and normalized according to the cell dry weight of the cultures (Figure 3A). The addition of a dodecane overlay enhanced the accumulation of sesquiterpenes as previously reported.[31] Additionally, we also demonstrated that it does not alter the distribution of the different products (Figure 3A). Cultures conducted with buffered (pH 7.4) or nonbuffered media reveal that the pH exerts a significant effect on the pattern of sesquiterpenes accumulated in the dodecane overlay: there is a concomitant reduction of nerolidol synthesis and a greater accumulation of farnesol at pH 7.4. With a nonbuffered minimal medium (SD), the final pH dropped to *ca* 3 after 120 h of culture. In such an acidic condition, Cope rearrangement can occur and convert farnesol to nerolidol.[43] In contrast, with a nonbuffered rich medium (YPA), the pH dropped to *ca* 5 at the end of the culture and the accumulation of nerolidol was limited, confirming the pH-dependent conversion of farnesol to nerolidol (Figure 3A). Surprisingly, the overall production of sesquiterpenes, including (+)-*epi*-α-bisabolol, per cell is lower in a complete medium (YPA) compared to minimal medium (SD), which might be attributed to a possible difference in the way methionine represses the expression of *ERG9* by the *MET3* promoter, leading to a change in the flux to FPP. However, when the total amount of (+)-*epi*-α-bisabolol produced per liter of culture is compared (Figure 3B), there is a 34% improvement of the (+)-*epi*-α-bisabolol quantity produced in YPA medium compared to the SD medium due to a higher cell density obtained in a rich medium.

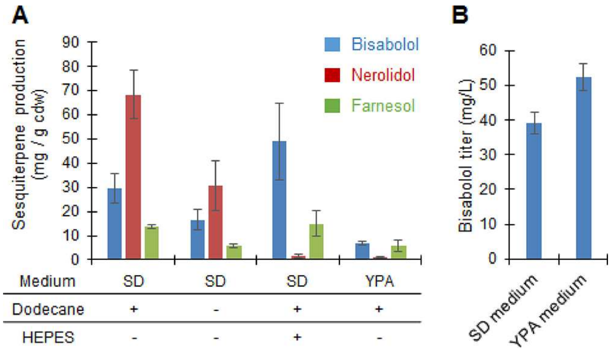

Figure 3. Production of sesquiterpenes by YBIS_01 strain cultured in different conditions. All cultures were performed in triplicate. (A) YBIS_01 sesquiterpene production with or without dodecane overlay, in nonbuffered conditions or buffered conditions, and SD or YPA media. The sesquiterpene production was normalized according to the cell dry weight. (B) (+)-*epi*-α-bisabolol titer in SD and YPA media.

Competing reactions by endogenous phosphatases such as DPP1 and LPP1 may decrease the production of (+)-*epi*-α-bisabolol by transforming part of the FPP to farnesol (Figure 2D).[45] To resolve this issue, we deleted DPP1 with or without adding a second copy of BBS, generating YBIS_05 (one BBS copy) and YBIS_06, (2 copies of BBS) from YBIS_01. The comparison between YBIS_01 and YBIS_05 indicates that the deletion of the DPP1 gene has a negligible effect on (+)-*epi*-α-bisabolol production (Figure 4). On the contrary, adding a second copy of the BBS gene significantly enhanced (+)-*epi*-α-bisabolol production (~70% increase) showing that further potential improvements, either at the level of quantity or specific activity of BBS, are still feasible.

(+)-epi-α-Bisabolol in Vivo Concentration Influences the Oxidized Metabolite Production. While the addition of dodecane increased the production of (+)-*epi*-α-bisabolol and isomers, we did not use this pulling effect for the production of the oxidized derivatives as it may decrease the presence of intracellular (+)-*epi*-α-bisabolol available for the CYP. The comparison between YBIS_05 and YBIS_06 for the production of hydroxylated derivatives by CYP2C9 and CYP2D6 is presented in Figure 5. Interestingly, in the absence

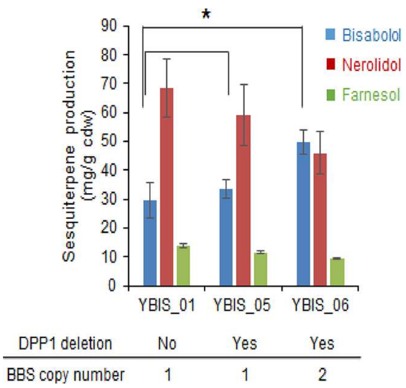

Figure 4. Comparison of the sesquiterpene production by YBIS_01, YBIS_05 (*DDP1* gene deletion), and YBIS_06 strains (*DDP1* gene deletion and one supplementary copy of the BBS encoding gene). All cultures were performed in triplicate in SD medium with a dodecane overlay spiked with nootkatone as the internal standard. Statistical comparison of (+)-*epi*-α-bisabolol production using a *t* test between YBIS_01 and YBIS_05, *p*-value = 0.17; YBIS_01 and YBIS_06, *p*-value = 0.0056.

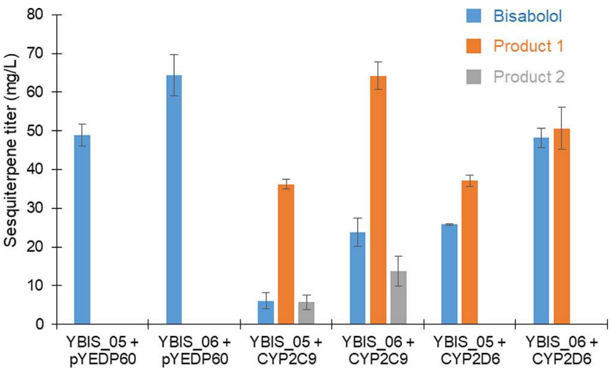

Figure 5. Effect of chassis improvement on accumulation of CYP2C9 and CYP2D6 products. The level of (+)-*epi*-α-bisabolol was varied in the strains by comparing YBIS_05 (1 integrated BBS copy) to YBIS_06 (2 integrated BBS copies).

of the pulling effect of dodecane, YBIS_06 produced only 32% more (+)-*epi*-α-bisabolol than YBIS_05 (compared to the 70% increase with dodecane, Figure 4), suggesting a partial inhibition of BBS by the product of the reaction, namely (+)-*epi*-α-bisabolol.

While *in vitro* assays with CYP2C9 gave three different products, only two of them were detected in the cultured cells. In the strain YBIS_05 + CYP2C9, the remaining level of (+)-*epi*-α-bisabolol indicates an 87% conversion of this precursor to its oxidized derivatives. This conversion yield dropped slightly to 77% in YBIS_06 + CYP2C9. Interestingly, an extra copy of the BBS encoding gene (YBIS_06 + CYP2C9) raised the quantity of oxidized products compared to YBIS_05 + CYP2C9 with a concomitant accumulation of (+)-*epi*-α-bisabolol. Indeed, 36 mg/L (+)-*epi*-α-bisabolol oxidized product 1 and 5.7 mg/L of product 2 are produced in YBIS_05 + CYP2C9 while 64 mg/L of (+)-*epi*-α-bisabolol oxidized product 1 and 13 mg/L of product 2 were synthesized YBIS_05 + CYP2C9. This demonstrates that the reaction promoted by CYP2C9 in YBIS_05 + CYP2C9 is not limiting. The conversion yields in YBIS_05 + CYP2D6 and YBIS_06 + CYP2D6 were, respectively, 59 and 51%, while the final titer of the (+)-*epi*-α-bisabolol oxidized product 1 reached 37 and 50 mg/L in YBIS_05 + CYP2D6 and YBIS_06 + CYP2D6, respectively. Hence, with CYP2D6, the difference of production of oxidized products suggests that the enzymatic step catalyzed by CYP2D6 was not completely limiting in YBIS_05 + CYP2D6.

The comparison between the strains YBIS_05 and YBIS_06 with both CYP2C9 and CYP2D6 also indicates that although none of the reactions catalyzed by the two CYPS are limiting, the *in vivo* efficiency of conversion of CYP2C9 is greater than that of CYP2D6. Alternatively, the diminution of the farnesol pool due to the second copy of BBS (Figure 4) could also be beneficial due to the possible change in the competition between the two substrates for the CYP. Thus, having a second copy of BBS is still beneficial for the accumulation of oxidized product by CYP2D6.

Product Purification and Structure Determination. For structural characterization of the oxidized molecules produced by CYP2B6, CYP2B11, CYP2C9, CYP2C18, and CYP2D6, and to circumvent the limit of resolution of the HPLC method, we turned to GC analyses with and without performing a trimethylsilylation derivatization reaction. (−)-α-Bisabolol was used as control. According to HPLC analysis, CYP2C18 and CYP2D6 yielded only one molecule, and the same pattern was found in GC−MS. Furthermore, their mass spectra (native product as well as the trimethylsilylated derivative) are identical (Figure S9). We can then assume that the products synthesized by CYP2C18 and CYP2D6 are identical. With CYP2C9, two products are also detected by HPLC and GC. The major compound produced by CYP2C9 is identical to the one synthesized by CYP2C18 and CYP2D6. For CYP2B6 and CYP2B11, the analysis of the oxidized products in GC and HPLC was difficult due to multiplicity of the products formed. However, the product profiles were distinguishable from those obtained with the other CYPs, indicating the presence of different products. The fractions isolated from YBIS_06 + CYP2B6 and YBIS_06 + CYP2B11 culture supernatant contained a complex mixture of oxidized sesquiterpene products potentially originating from both (+)-*epi*-α-bisabolol and/or farnesol and additional endogenous contaminants, which could not be separated prior to NMR characterization. We thus pursued the purification of the products synthesized by CYP2C9 and CYP2D6 using the strain YBIS_06 transformed by the corresponding high copy plasmids. CYP2C18, which probably produces the same oxidized (+)-*epi*-α-bisabolol derivative as CYP2D6 (and in lower yield), was not further analyzed. We noted that, even in the absence of a dodecane layer, more than 80% of the oxidized products of (+)-*epi*-α-bisabolol accumulated in the culture broth, while most of the sesquiterpenes remained trapped within the cell (Figure S10). The different cell/medium partition behavior between (+)-*epi*-α-bisabolol and its oxidized products may be in part due to the presence of an endogenous yeast transporter that could excrete the oxidized products but not (+)-*epi*-α-bisabolol.

After isolation of the oxidized products recovered from the culture supernatants of YBIS_06 + CYP2D6 and YBIS_06 + CYP2C9, sufficient amounts of oxidized (+)-*epi*-α-bisabolol were purified and recovered for NMR analysis. One single oxidized product was found in the purified fraction obtained from the YBIS_06 + CYP2D6 culture, and two in the fraction generated with YBIS_06 + CYP2C9. NMR analysis confirmed that both CYP2D6 and CYP2C9 produced new to nature molecules derived from (+)-*epi*-α-bisabolol (Figure 6, Figure S11, and Table S3). The ^{1}H spectrum of 14-hydroxy-(+)-*epi*-α-bisabolol produced by CYP2D6 displays only three signals attributed to methyl groups (H-13 at 1.69, H-12 at 1.63, and H-15 at 1.15 ppm). It is noteworthy that the disappearance of the H-14 methyl singlet of (+)-*epi*-α-bisabolol at 1.64 ppm is combined with the appearance of the H-14 methylene signal at 4.01 ppm of 14-hydroxy-(+)-*epi*-α-bisabolol. Similarly, the ^{13}C spectrum of 14-hydroxy-(+)-*epi*-α-bisabolol reveals only three methyl signals (28.7, 24.0, and 17.7 ppm corresponding to C-13, C-15, and C-12, respectively) combined with the additional C-14 methylene signal at 67.2 ppm. In addition to 14-hydroxy-(+)-*epi*-α-bisabolol, NMR spectra of the mixture produced by CYP2C9 also highlighted some traces of a second metabolite. It is characterized by the presence of two new signals at 5.41 (triplet, H-3) and 5.38 ppm (broad singlet, H-10; unblinded compared to the H-10 signals of (+)-*epi*-α-bisabolol and 14-hydroxy-(+)-*epi*-α-bisabolol) correlating with two methyne signals (CH═) at 126.1 and 120.6 ppm, respectively, and combined with at least two putative methyl singlets (1.63/23.3 and 1.11/24.1 ppm, H/C-14 and 15 pairs, respectively) (Table S3). This led us to presume that the minor product is 9-hydroxy-(+)-*epi*-α-bisabolol, but we cannot exclude completely that it corresponds to 8-hydroxy-(+)-*epi*-α-bisabolol.

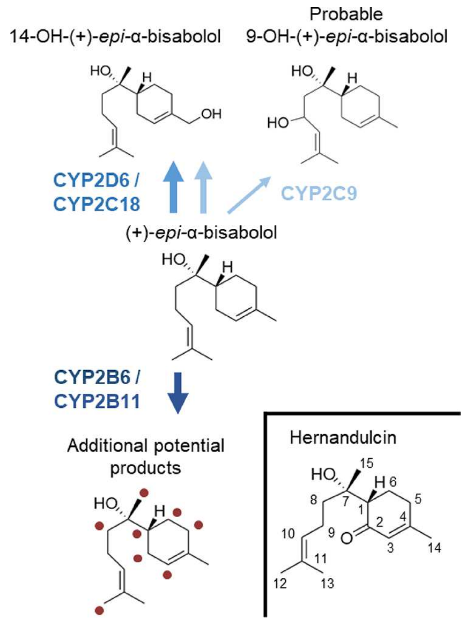

Figure 6. Chemical structures of the newly generated molecules. CYP2D6 produces 14-hydroxy-(+)-*epi*-α-bisabolol while CYP2C9 produces 80% of 14-hydroxy-(+)-*epi*-α-bisabolol and 20% of a second additional hydroxylated (+)-*epi*-α-bisabolol derivative, most probably 9-hydroxy-(+)-*epi*-α-bisabolol. The red dots on the (+)-*epi*-α-bisabolol molecule indicate the other positions that could be hydroxylated in CYP2B6 and CYP2B11 although the original molecules could not be fully characterized by NMR.

It is worth noting that at least three CYPs (CYP2C9, CYP2C18, and CYP2D6) produce 14-hydroxy-(+)-*epi*-α-bisabolol. Considering their known difference in substrate specificity,[46] it may be tempting to hypothesize that, while various CYPs have different binding sites and may promote various positioning of the substrate within the active site, the hydroxylation at C-14 is thermodynamically favored over the other positions. The minor product formed by CYP2C9, most probably 9-hydroxy-(+)-*epi*-α-bisabolol, shows an attack of the substrate at a completely opposite position compared to the 14-hydroxy-(+)-*epi*-α-bisabolol, which probably signs a different mode of binding or, alternatively, the use of a second substrate channel for entering CYP2C9 that is known to alter oxidation specificity.[47] Overall, for the products of CYP2D6, CYP2C18, and CYP2C9 the hydroxyl group was not introduced on the C-2 carbon, the one that possesses the carbonyl function in hernandulcin. However, because other minor products are formed with CYP2B6 or CYP2B11, we cannot exclude that this hydroxy derivative is indeed present in the complex mixture. Further studies such as lowering the farnesol content and increasing the amount of (+)-*epi*-α-bisabolol formed should help in the identification of these new metabolites.

■ DISCUSSION

In this paper, we developed an *in vivo* screening strategy to discover oxidized derivatives of (+)-*epi*-α-bisabolol such as hernandulcin (Figure 6), a powerful sweetener naturally produced by *Lippia dulcis*. Although human CYPs have already been efficiently used for metabolic engineering purposes such as the complete hydrocortisone biosynthesis,[48] there is no demonstration, to our knowledge, of the use of human CYPs in diverting plant terpene metabolism. Therefore, rather than searching for the right, specific, CYP candidate in *Lippia dulcis*, we deliberately screened an animal drug metabolism CYP enzyme library. Our rationale was based on the facts that (i) the oxidizing enzymes from *L. dulcis* were not yet identified and no CYPs were characterized with (+)-*epi*-α-bisabolol as substrate, and (ii) drug metabolism CYP isoforms are constantly exposed to terpenes from natural sources via food supply and could well have evolved to oxidize these compounds prior to their excretion. Furthermore, comparative studies of plant and animal CYP metabolisms, which focused on inhibition/competition experiments, identified inhibitor molecules from plants but rarely considered them as potential substrates.

Out of the 25 screened CYPs, we identified 5 CYPs that produced hydroxylated derivatives of (+)-*epi*-α-bisabolol from the CYP2 family (CYP2B6, CYP2B11, CYP2C9, CYP2C18, and CYP2D6) and 1 from the CYP1 family (CYP1A1), which was actually more active on farnesol. The fact that mostly CYP2 family isoforms were identified corroborates existing data on their role in oxidizing monoterpenes[49] and sesquiterpenes.[50] We can thus hypothesize that structural elements conserved in the CYP2 family favor the recognition of this class of C_{15} molecules. Wider structure/activity relationship studies may help to decipher which structural motifs are responsible for this recognition in the CYP2 family, especially considering the quite strong regiospecificity of CYP2D6, CYP2C18, and CYP2C9 for the position C-14.

Some available bioinformatics tools seek the prediction of human CYPs specificities due to their main contribution in drug metabolism.[51] We then assessed two different tools, namely FAME3 and xenosite to evaluate their accuracy in predicting if (+)-*epi*-α-bisabolol could be a substrate of the CYP tested.[52,53] Their results are presented in Figure S12. Fame3 output is the overall metabolism from human CYPs, and the 14-hydroxy-(+)-*epi*-α-bisabolol that is the major product of CYP2D6, CYP2C18, and CYP2C9 has a score that predicts it at the third probable metabolite. The 9-

hydroxy-(+)-*epi*-α-bisabolol produced by CYP2C9 is even less successfully considered. Regarding the Xenosite tool, it aims at predicting the metabolites from each individual human CYP. Its prediction with CYP2D6 shows that 14-hydroxy-(+)-*epi*-α-bisabolol is indeed the favored product. However, additional metabolites are proposed, whereas from the yeast *in vivo* production we do not detect such products. For CYP2C9, 14-hydroxy-(+)-*epi*-α-bisabolol is found as well, but the 9-hydroxy-(+)-*epi*-α-bisabolol production is not identified and multiple additional metabolites are expected. Additionally, some CYPs such as CYP3A4 or CYP2C8 are proposed to convert (+)-*epi*-α-bisabolol to a wide range of new molecules while we do not observe this pattern in our *in vivo* screening. Overall this demonstrates that validating the human CYPs activities and specificities is a necessary step.

Although the screening was implemented in a strain adequate for FPP and (+)-*epi*-α-bisabolol synthesis, both (+)-*epi*-α-bisabolol and farnesol were produced in similar amounts. *In vitro* testing of the positive hits from our library with both substrates revealed that all identified CYPs accepted both sesquiterpenes as substrates. However, when product purification on a subset of molecules was carried out from *in vivo* experiments, only (+)-*epi*-α-bisabolol oxidized products were purified. Although CYP2E1 and CYP2C19 were also shown to oxidize farnesol *in vitro*,[50] we could not find any evidence for the production of such molecules with both isoforms in our *in vivo* experiments. The low farnesol hydroxylation activities in the selected CYP2 isoforms could be due to a weaker affinity or lower turnover number for farnesol than (+)-*epi*-α-bisabolol or, in the case of CYP2E1, potential ethanol inhibition of the CYP activity.[50] Alternatively, additional hurdles such as poor substrate accessibility inside yeast cells or a different compartmentalization of the two substrates might also account for the lack of farnesol metabolism.

Remarkably, most of the (+)-*epi*-α-bisabolol metabolites were secreted into the culture medium. Understanding whether passive or active transport or free diffusion causes this phenomenon would be valuable for further improvement of our chassis strain and would be also of interest to potentially excrete other types of molecules. The recent discovery of the positive role of heterologous expression of human transporters in excreting fatty alcohols from yeast is a strong advocacy for the search of potential transporter gene candidates that would increase product efflux to the culture medium.[54] Such efflux pumps not only could help metabolic engineering reach better titers by finding highly active transporters but may also, if inactivated, avoid the escape of intermediates prior to their reaction with specific enzymes in synthetic pathways.

Our data show accumulation of oxidized products of (+)-*epi*-α-bisabolol up to 64 mg/L without any enzyme engineering refinement strategy. Further improvements of these new metabolic pathways may be achievable by a finer tuning of the fluxes toward the side reactions,[55] or alternatively, by CYP engineering which are not fully dedicated and evolved for this type of reaction. Our metabolic engineering strategy can now be extended to additional monoterpenes, sesquiterpenes, or diterpenes backbones or even other classes of molecules such as flavonoids as some human CYPs are also known to metabolize them.[56] Plant secondary metabolism includes thousands of chemical backbones, while human CYPs metabolize 70−80% of clinical drugs.[25] Combining these two characteristic features could open up a tremendous chemical space of active compounds. The remaining challenge of such studies would be the adjustment of relevant screens for biological activities of the newly generated molecules.

■ CONCLUSION

The approach consisting of screening potentially new enzyme activities directly *in vivo*, in an optimized chassis, possesses several advantages when it comes to metabolic engineering. On the one hand, all enzymes identified in the first place are expressed in conditions that are relevant for product accumulation inside biologically active cells. While sometimes discrepancies between the enzymatic reactions and the production in whole cells may exist,[57] *in vivo* screening may allow a much higher throughput when dealing with cumbersome enzymes such as CYPs that are harder to evaluate from the *in vitro* point of view due to their endoplasmic reticulum targeting and tedious methods to isolate microsomal fractions. Even if our strategy, different from the classical enzyme mining from the natural host, did not succeed in hernandulcin production, we clearly demonstrate the validity of our design in expanding the scope of known chemicals and exemplified, using (+)-*epi*-α-bisabolol, the generation of completely new molecules. Given the biological activities of bisabolol (anti-inflammatory, potentiating antibiotics) and hernandulcin (sweetener), these novel molecules may exhibit interesting properties that have yet to be explored. To further expand the diversity of accessible molecules after hydroxylation, the addition of plant alcohol dehydrogenases to the system may enable the formation of keto groups in the hydroxylated sesquiterpene, mimicking potential biosynthetic pathways existing in plants[8,58] and potentially allowing access to hernandulcin when a CYP targeting the carbon at the C-2 position will be discovered.

■ ASSOCIATED CONTENT

Supporting Information

The Supporting Information is available free of charge at

Library of tested CYPs; primers used in this study; NMR data; chromatograms; other figures and tables as mentioned in the text (PDF)

■ AUTHOR INFORMATION

Corresponding Authors

Magali Remaud-Siméon − *TBI, Université de Toulouse, CNRS, INRAE, INSA, Toulouse, France;* orcid.org/0000-0002-2658-672X; Email: magali.remaud@insa-toulouse.fr

Gilles Truan − *TBI, Université de Toulouse, CNRS, INRAE, INSA, Toulouse, France;* orcid.org/0000-0002-3560-8302; Email: gilles.truan@insa-toulouse.fr

Authors

Arthur Sarrade-Loucheur − *TBI, Université de Toulouse, CNRS, INRAE, INSA, Toulouse, France;* orcid.org/0000-0003-3505-2532

Dae-Kyun Ro − *Department of Biological Sciences, University of Calgary, Calgary, Canada;* orcid.org/0000-0003-1288-5347

Régis Fauré − *TBI, Université de Toulouse, CNRS, INRAE, INSA, Toulouse, France;* orcid.org/0000-0002-5107-9009

Author Contributions

M.R.S. and G.T. conceived the study. A.S.L., M.R.S., and G.T. designed the experiments. A.S.L. performed all biological and analytical experiments with the help of R.F. for the purification of products; R.F. performed the NMR acquisition and analysis. D.K.R. participated in the design of the early stages of the project and provided the EPY300 strain. A.S.L. wrote the first draft of the manuscript, which was then revised by all authors.

Notes

The authors declare no competing financial interest.

■ ACKNOWLEDGMENTS

We acknowledge Thomas Lautier for the supply of microsomal fractions of CYP2B11. NMR analyses were performed using facilities at MetaToul (Metabolomics & Fluxomics Facilities, Toulouse, France, www.metatoul.fr), which is part of the national infrastructure MetaboHUB (The French National infrastructure for metabolomics and fluxomics, www.metabohub.fr) and is supported by grants from the Région Midi-Pyrénées, the European Regional Development Fund, SICOVAL, IBiSa-France, CNRS, and INRA. A.S.L. received a Ph.D. fellowship from the French minister of education research. Edern Cahoreau, staff member of the MetaToul platform, is gratefully acknowledged for the technical support. Also we would like to thank the ICEO facility dedicated to enzyme screening and discovery, part of the Integrated Screening Platform of Toulouse (PICT, IBiSA), for providing access to GC-FID−MS.

■ NOTATION

BBS	(+)-*epi*-α-bisabolol synthase
CYP	cytochrome P450
CPR	NADPH cytochrome P450 reductase
FID	flame ionization detector
FPP	farnesyl pyrophosphate
GC	gas chromatography
HPLC	high pressure liquid chromatography
MS	mass spectrometry
MW	molecular weight
OD	optical density
UV	ultraviolet

■ REFERENCES

(1) Liao, P., Hemmerlin, A., Bach, T. J., and Chye, M.-L. (2016) The potential of the mevalonate pathway for enhanced isoprenoid production. *Biotechnol. Adv. 34*, 697−713.

(2) Chiu, C. C., Keeling, C. I., and Bohlmann, J. (2018) Monoterpenyl esters in juvenile mountain pine beetle and sex-specific release of the aggregation pheromone trans-verbenol. *Proc. Natl. Acad. Sci. U. S. A. 115*, 3652−3657.

(3) Umehara, M., Hanada, A., Yoshida, S., Akiyama, K., Arite, T., Takeda-Kamiya, N., Magome, H., Kamiya, Y., Shirasu, K., Yoneyama, K., Kyozuka, J., and Yamaguchi, S. (2008) Inhibition of shoot branching by new terpenoid plant hormones. *Nature 455*, 195−200.

(4) Kramer, R., and Abraham, W.-R. (2012) Volatile sesquiterpenes from fungi: what are they good for? *Phytochem. Rev. 11*, 15−37.

(5) Kim, S., Jung, E., Kim, J.-H., Park, Y.-H., Lee, J., and Park, D. (2011) Inhibitory effects of (−)-α-bisabolol on LPS-induced inflammatory response in RAW264.7 macrophages. *Food Chem. Toxicol. 49*, 2580−2585.

(6) Vickers, C. E., Williams, T. C., Peng, B., and Cherry, J. (2017) Recent advances in synthetic biology for engineering isoprenoid production in yeast. *Curr. Opin. Chem. Biol. 40*, 47−56.

(7) Itkin, M., Davidovich-Rikanati, R., Cohen, S., Portnoy, V., Doron-Faigenboim, A., Oren, E., Freilich, S., Tzuri, G., Baranes, N., Shen, S., Petreikov, M., Sertchook, R., Ben-Dor, S., Gottlieb, H., Hernandez, A., Nelson, D. R., Paris, H. S., Tadmor, Y., Burger, Y., Lewinsohn, E., Katzir, N., and Schaffer, A. (2016) The biosynthetic pathway of the nonsugar, high-intensity sweetener mogroside V from *Siraitia grosvenorii*. *Proc. Natl. Acad. Sci. U. S. A. 113*, E7619−E7628.

(8) Ringer, K. L., Davis, E. M., and Croteau, R. (2005) Monoterpene metabolism. Cloning, expression, and characterization of (−)-isopiperitenol/(−)-carveol dehydrogenase of peppermint and spearmint. *Plant Physiol. 137*, 863−872.

(9) Maimone, T. J., and Baran, P. S. (2007) Modern synthetic efforts toward biologically active terpenes. *Nat. Chem. Biol. 3*, 396.

(10) Polakowski, T., Stahl, U., and Lang, C. (1998) Overexpression of a cytosolic hydroxymethylglutaryl-CoA reductase leads to squalene accumulation in yeast. *Appl. Microbiol. Biotechnol. 49*, 66−71.

(11) Paddon, C. J., Westfall, P. J., Pitera, D. J., Benjamin, K., Fisher, K., McPhee, D., Leavell, M. D., Tai, A., Main, A., Eng, D., Polichuk, D. R., Teoh, K. H., Reed, D. W., Treynor, T., Lenihan, J., Jiang, H., Fleck, M., Bajad, S., Dang, G., Dengrove, D., Diola, D., Dorin, G., Ellens, K. W., Fickes, S., Galazzo, J., Gaucher, S. P., Geistlinger, T., Henry, R., Hepp, M., Horning, T., Iqbal, T., Kizer, L., Lieu, B., Melis, D., Moss, N., Regentin, R., Secrest, S., Tsuruta, H., Vazquez, R., Westblade, L. F., Xu, L., Yu, M., Zhang, Y., Zhao, L., Lievense, J., Covello, P. S., Keasling, J. D., Reiling, K. K., Renninger, N. S., and Newman, J. D. (2013) High-level semi-synthetic production of the potent antimalarial artemisinin. *Nature 496*, 528−532.

(12) Peng, B., Plan, M. R., Chrysanthopoulos, P., Hodson, M. P., Nielsen, L. K., and Vickers, C. E. (2017) A squalene synthase protein degradation method for improved sesquiterpene production in Saccharomyces cerevisiae. *Metab. Eng. 39*, 209−219.

(13) Peng, B., Plan, M. R., Carpenter, A., Nielsen, L. K., and Vickers, C. E. (2017) Coupling gene regulatory patterns to bioprocess conditions to optimize synthetic metabolic modules for improved sesquiterpene production in yeast. *Biotechnol. Biofuels 10*, No. 0728-x, DOI: 10.1186/s13068-017-0728-x.

(14) Zhu, F., Zhong, X., Hu, M., Lu, L., Deng, Z., and Liu, T. (2014) In vitro reconstitution of mevalonate pathway and targeted engineering of farnesene overproduction in *Escherichia coli*. *Biotechnol. Bioeng. 111*, 1396−1405.

(15) Aschenbrenner, A.-K., Kwon, M., Conrad, J., Ro, D.-K., and Spring, O. (2016) Identification and characterization of two bisabolene synthases from linear glandular trichomes of sunflower (*Helianthus annuus L., Asteraceae*). *Phytochemistry 124*, 29−37.

(16) Moses, T., Pollier, J., Faizal, A., Apers, S., Pieters, L., Thevelein, J. M., Geelen, D., and Goossens, A. (2015) Unraveling the Triterpenoid Saponin Biosynthesis of the African Shrub *Maesa lanceolata*. *Mol. Plant 8*, 122−135.

(17) Arendt, P., Pollier, J., Callewaert, N., and Goossens, A. (2016) Synthetic biology for production of natural and new-to-nature terpenoids in photosynthetic organisms. *Plant J. 87*, 16−37.

(18) Fukushima, E. O., Seki, H., Sawai, S., Suzuki, M., Ohyama, K., Saito, K., and Muranaka, T. (2013) Combinatorial biosynthesis of legume natural and rare triterpenoids in engineered yeast. *Plant Cell Physiol. 54*, 740−749.

(19) Moses, T., Pollier, J., Almagro, L., Buyst, D., Van Montagu, M., Pedreño, M. A., Martins, J. C., Thevelein, J. M., and Goossens, A. (2014) Combinatorial biosynthesis of sapogenins and saponins in *Saccharomyces cerevisiae* using a C-16α hydroxylase from *Bupleurum falcatum*. *Proc. Natl. Acad. Sci. U. S. A. 111*, 1634−1639.

(20) Andersen-Ranberg, J., Kongstad, K. T., Nielsen, M. T., Jensen, N. B., Pateraki, I., Bach, S. S., Hamberger, B., Zerbe, P., Staerk, D., Bohlmann, J., Møller, B. L., and Hamberger, B. (2016) Expanding the landscape of diterpene structural diversity through stereochemically controlled combinatorial biosynthesis. *Angew. Chem., Int. Ed. 55*, 2142−2146.

(21) Bian, G., Han, Y., Hou, A., Yuan, Y., Liu, X., Deng, Z., and Liu, T. (2017) Releasing the potential power of terpene synthases by a robust precursor supply platform. *Metab. Eng. 42*, 1−8.

(22) Compadre, C. M., Hussain, R. A., Lopez de Compadre, R. L., Pezzuto, J. M., and Kinghorn, A. D. (1987) The intensely sweet sesquiterpene hernandulcin: isolation, synthesis, characterization, and preliminary safety evaluation. *J. Agric. Food Chem. 35*, 273−279.

(23) Mori, K., and Kato, M. (1986) Synthesis of (6S, 1'S)-(+)-hernandulcin, a sweetner, and its stereoisomers. *Tetrahedron 42*, 5895−5900.

(24) Attia, M., Kim, S.-U., and Ro, D.-K. (2012) Molecular cloning and characterization of (+)-*epi*-α-bisabolol synthase, catalyzing the first step in the biosynthesis of the natural sweetener, hernandulcin, in *Lippia dulcis*. *Arch. Biochem. Biophys. 527*, 37−44.

(25) Zanger, U. M., and Schwab, M. (2013) Cytochrome P450 enzymes in drug metabolism: Regulation of gene expression, enzyme activities, and impact of genetic variation. *Pharmacol. Ther. 138*, 103−141.

(26) Pompon, D., Louerat, B., Bronine, A., and Urban, P. (1996) Yeast expression of animal and plant P450s in optimized redox environments. *Methods Enzymol. 272*, 51−64.

(27) Brehm-Stecher, B. F., and Johnson, E. A. (2003) Sensitization of *Staphylococcus aureus* and *Escherichia coli* to antibiotics by the sesquiterpenoids nerolidol, farnesol, bisabolol, and apritone. *Antimicrob. Agents Chemother. 47*, 3357−3360.

(28) Ganzera, M., Schneider, P., and Stuppner, H. (2006) Inhibitory effects of the essential oil of chamomile (*Matricaria recutita L.*) and its major constituents on human cytochrome P450 enzymes. *Life Sci. 78*, 856−861.

(29) Lautier, T., Urban, P., Loeper, J., Jezequel, L., Pompon, D., and Truan, G. (2016) Ordered chimerogenesis applied to CYP2B P450 enzymes. *Biochim. Biophys. Acta, Gen. Subj. 1860*, 1395−1403.

(30) Brachmann, C. B., Davies, A., Cost, G. J., Caputo, E., Li, J., Hieter, P., and Boeke, J. D. (1998) Designer deletion strains derived from *Saccharomyces cerevisiae* S288C: A useful set of strains and plasmids for PCR-mediated gene disruption and other applications. *Yeast 14*, 115−132.

(31) Nguyen, T.-D., MacNevin, G., and Ro, D.-K. (2012) De novo synthesis of high-value plant sesquiterpenoids in yeast, in *Methods in Enzymology*, pp 261−278, Elsevier.

(32) Ro, D.-K., Paradise, E. M., Ouellet, M., Fisher, K. J., Newman, K. L., Ndungu, J. M., Ho, K. A., Eachus, R. A., Ham, T. S., Kirby, J., Chang, M. C. Y., Withers, S. T., Shiba, Y., Sarpong, R., and Keasling, J. D. (2006) Production of the antimalarial drug precursor artemisinic acid in engineered yeast. *Nature 440*, 940−943.

(33) Xie, W., Liu, M., Lv, X., Lu, W., Gu, J., and Yu, H. (2014) Construction of a controllable β-carotene biosynthetic pathway by decentralized assembly strategy in *Saccharomyces cerevisiae*. *Biotechnol. Bioeng. 111*, 125−133.

(34) Xie, W., Ye, L., Lv, X., Xu, H., and Yu, H. (2015) Sequential control of biosynthetic pathways for balanced utilization of metabolic intermediates in *Saccharomyces cerevisiae*. *Metab. Eng. 28*, 8−18.

(35) Urban, P., Cullin, C., and Pompon, D. (1990) Maximizing the expression of mammalian cytochrome P-450 monooxygenase activities in yeast cells. *Biochimie 72*, 463−472.

(36) Gietz, R. D., and Schiestl, R. H. (2007) Frozen competent yeast cells that can be transformed with high efficiency using the LiAc/SS carrier DNA/PEG method. *Nat. Protoc. 2*, 1.

(37) Gietz, D., St Jean, A., Woods, R. A., and Schiestl, R. H. (1992) Improved method for high efficiency transformation of intact yeast cells. *Nucleic Acids Res. 20*, 1425.

(38) Gueldener, U., Heinisch, J., Koehler, G. J., Voss, D., and Hegemann, J. H. (2002) A second set of loxP marker cassettes for Cre-mediated multiple gene knockouts in budding yeast. *Nucleic Acids Res. 30*, No. e23.

(39) Othman, S., Mansuy-Mouries, V., Bensoussan, C., Battioni, P., and Mansuy, D. (2000) Hydroxylation of diclofenac: an illustration of the complementary roles of biomimetic metalloporphyrin catalysts and yeasts expressing human cytochromes P450 in drug metabolism studies. *C. R. Acad. Sci., Ser. IIc: Chim. 3*, 751−755.

(40) Adams, R. P., Weerasooriya, A., and Gao, M. (2014) Comparison of volatile leaf terpenoids from *Lippia dulcis* (*Verbenaceae*) obtained by steam distillation and pentane liquid extraction. *Phytologia 96*, 252−259.

(41) Demarque, D. P., Crotti, A. E., Vessecchi, R., Lopes, J. L., and Lopes, N. P. (2016) Fragmentation reactions using electrospray ionization mass spectrometry: an important tool for the structural elucidation and characterization of synthetic and natural products. *Nat. Prod. Rep. 33*, 432−455.

(42) Kampranis, S. C., and Makris, A. M. (2012) Developing a yeast cell factory for the production of terpenoids. *Comput. Struct. Biotechnol. J. 3*, No. e201210006.

(43) Hu, Y., Zhou, Y. J., Bao, J., Huang, L., Nielsen, J., and Krivoruchko, A. (2017) Metabolic engineering of *Saccharomyces cerevisiae* for production of germacrene A, a precursor of beta-elemene. *J. Ind. Microbiol. Biotechnol. 44*, 1065−1072.

(44) Scalcinati, G., Knuf, C., Partow, S., Chen, Y., Maury, J., Schalk, M., Daviet, L., Nielsen, J., and Siewers, V. (2012) Dynamic control of gene expression in *Saccharomyces cerevisiae* engineered for the production of plant sesquitepene α-santalene in a fed-batch mode. *Metab. Eng. 14*, 91−103.

(45) Faulkner, A., Chen, X., Rush, J., Horazdovsky, B., Waechter, C. J., Carman, G. M., and Sternweis, P. C. (1999) The LPP1 and DPP1 gene products account for most of the isoprenoid phosphate phosphatase activities in *Saccharomyces cerevisiae*. *J. Biol. Chem. 274*, 14831−14837.

(46) Tornio, A., and Backman, J. T. (2018) Chapter One−Cytochrome P450 in Pharmacogenetics: An Update, in *Advances in Pharmacology* (Brøsen, K., and Damkier, P., Eds.), pp 3−32, Academic Press.

(47) Urban, P., Lautier, T., Pompon, D., and Truan, G. (2018) Ligand access channels in cytochrome P450 enzymes: A Review. *Int. J. Mol. Sci. 19*, 1617.

(48) Szczebara, F. M., Chandelier, C., Villeret, C., Masurel, A., Bourot, S., Duport, C., Blanchard, S., Groisillier, A., Testet, E., Costaglioli, P., Cauet, G., Degryse, E., Balbuena, D., Winter, J., Achstetter, T., Spagnoli, R., Pompon, D., and Dumas, B. (2003) Total biosynthesis of hydrocortisone from a simple carbon source in yeast. *Nat. Biotechnol. 21*, 143−149.

(49) Shah, M. B., Wilderman, P. R., Liu, J., Jang, H.-H., Zhang, Q., Stout, C. D., and Halpert, J. R. (2015) Structural and biophysical characterization of human cytochromes P450 2B6 and 2A6 bound to volatile hydrocarbons: Analysis and comparison. *Mol. Pharmacol. 87*, 649−659.

(50) DeBarber, A. E., Bleyle, L. A., Roullet, J.-B. O., and Koop, D. R. (2004) ω-Hydroxylation of farnesol by mammalian cytochromes P450. *Biochim. Biophys. Acta, Mol. Cell Biol. Lipids 1682*, 18−27.

(51) Tyzack, J. D., and Kirchmair, J. (2019) Computational methods and tools to predict cytochrome P450 metabolism for drug discovery. *Chem. Biol. Drug Des. 93*, 377−386.

(52) Šícho, M., Stork, C., Mazzolari, A., de Bruyn Kops, C., Pedretti, A., Testa, B., Vistoli, G., Svozil, D., and Kirchmair, J. (2019) FAME 3: Predicting the sites of Metabolism in Synthetic Compounds and Natural Products for Phase 1 and Phase 2 Metabolic Enzymes. *J. Chem. Inf. Model. 59*, 3400−3412.

(53) Zaretzki, J., Matlock, M., and Swamidass, S. J. (2013) XenoSite: Accurately Predicting CYP-Mediated Sites of Metabolism with Neural Networks. *J. Chem. Inf. Model. 53*, 3373−3383.

(54) Hu, Y., Zhu, Z., Nielsen, J., and Siewers, V. (2018) Heterologous transporter expression for improved fatty alcohol secretion in yeast. *Metab. Eng. 45*, 51−58.

(55) Albertsen, L., Chen, Y., Bach, L. S., Rattleff, S., Maury, J., Brix, S., Nielsen, J., and Mortensen, U. H. (2011) Diversion of Flux toward Sesquiterpene Production in *Saccharomyces cerevisiae* by Fusion of Host and Heterologous Enzymes. *Appl. Environ. Microbiol. 77*, 1033−1040.

(56) Androutsopoulos, V. P., Papakyriakou, A., Vourloumis, D., and Spandidos, D. A. (2011) Comparative CYP1A1 and CYP1B1 substrate and inhibitor profile of dietary flavonoids. *Bioorg. Med. Chem. 19*, 2842−2849.

(57) Schaub, P., Yu, Q., Gemmecker, S., Poussin-Courmontagne, P., Mailliot, J., McEwen, A. G., Ghisla, S., Al-Babili, S., Cavarelli, J., and Beyer, P. (2012) On the Structure and Function of the Phytoene Desaturase CRTI from Pantoea ananatis, a Membrane-Peripheral and FAD-Dependent Oxidase/Isomerase. *PLoS One 7*, No. e39550.
(58) Okamoto, S., Yu, F., Harada, H., Okajima, T., Hattan, J., Misawa, N., and Utsumi, R. (2011) A short-chain dehydrogenase involved in terpene metabolism from Zingiber zerumbet. *FEBS J. 278*, 2892−2900.